

We are IntechOpen, the world's leading publisher of Open Access books Built by scientists, for scientists

6,900

Open access books available

186,000

International authors and editors

200M

Downloads

Our authors are among the

154

Countries delivered to

TOP 1%

most cited scientists

12.2%

Contributors from top 500 universities



WEB OF SCIENCE™

Selection of our books indexed in the Book Citation Index
in Web of Science™ Core Collection (BKCI)

Interested in publishing with us?
Contact book.department@intechopen.com

Numbers displayed above are based on latest data collected.
For more information visit www.intechopen.com



Electronic and Transport Properties of Defected Graphene Nanoribbons

Narjes Gorjizadeh¹, Yoshiyuki Kawazoe¹ and Amir A. Farajian²

¹Tohoku University,

²Wright State University,

¹Japan

²U.S.A.

1. Introduction

Graphene nanoribbons, quasi-one-dimensional structures of carbon, are fascinating materials. These structures can be constructed as strips of graphene sheet, the two dimensional honeycomb lattice of carbon with sp^2 hybridization. Geometrically two main types of slice can be cut from a graphene sheet, with zigzag edge and armchair edge (Niimi05; Kobayashi05). The edge geometry is the key parameter which determines the electronic properties of the nanoribbons. Although the two-dimensional graphene is a zero band-gap semi-metal, electronic structure of nanoribbons depend on their edge geometry (Saito92; Klein94; Fujita96; Son06a). A simple tight-binding model with one orbital per atom predicts that zigzag nanoribbons are metallic. But density functional calculations shows that all graphene nanoribbons are semiconductors at their ground state with band gaps which depend on their width and edge geometry, closing at infinite width, i. e. infinite graphene. Moreover, the electronic structure of graphene nanoribbons can be modified by chemical functionalization, such as functionalization by various atomic species or by functional groups (Maruyama04a; Gunlycke07; Hod07; Gorjizadeh08). A large variety of electronic and magnetic properties, such as semiconducting with a wide range of band gap, metallic, ferromagnetic, antiferromagnetic, half-metallic, half-semiconducting, can be obtained by chemical modifications of the nanoribbons. Modification of the edge or using an adsorbate or substitution of carbons of the nanoribbon with an appropriate host are different options of functionalizations of these materials. These properties, along with the ballistic electronic transport, and the quantum Hall effect (Novoselov05a; Zhang05) and high carrier mobility (Novoselov05a) cause these quasi-1D materials to be promising candidates for nanoelectronics applications (Novoselov04b; Son06b; Obradovic06; Li08; Hod09; Zhu10). Various junctions can be constructed by connecting nanoribbons of different widths and types with perfect atomic interface, and electronic device can be integrated on them by selective chemical functionalization on a single nanoribbon sheet (Huang07; Yan07; Gorjizadeh08).

In order to achieve their potential for these applications it is essential to have a better understanding of the electronic structure of graphene nanoribbons and have ability to control them. From a practical point of view, when nanoribbons are fabricated

experimentally, they will have some structural defects. Vacancy and adatom–vacancy defects are among the most probable ones (Hashimoto04). These defects should be taken into account in practical aspects of the electronic transport in nanodevices based on graphene nanoribbons. In this chapter we will discuss the effects of defects in quantum conductance of graphene nanoribbons. In next section we will review the geometry of armchair and zigzag nanoribbons. Dependence of their electronic properties on the width and edge shape will be discussed. Then, an overview of nonequilibrium Green's function formalism (NEGF) for calculation of quantum conductance will be presented. After that the results of conductance calculation of armchair and zigzag nanoribbons with some structural defects such as vacancies and adatom–vacancies will be discussed using NEGF techniques combined with a four-orbitals-per-atom tight-binding method. We will then show dependence of the conductance on the width of nanoribbons and the position of the defects and their distance from the edge of the nanoribbons.

2. Geometry and electronic structure of graphene nanoribbons

There are two types of nanoribbons, based on their edge shapes, called zigzag and armchair edges (Saito92). The width of the nanoribbons is labeled by an integer, N , which stands for the number of carbon dimers counted from one edge toward the other edge of armchair nanoribbons and the number of zigzag lines for zigzag nanoribbons. Figure 1 shows the two types of nanoribbons with their width indices. The dotted rectangle in this figure represents the unit cell of the nanoribbons. Nanoribbon is like an unrolled carbon nanotube (CNTs). The difference between carbon nanotubes and nanoribbons is the periodic boundary condition. Instead of a seamless tube, nanoribbon has two open boundaries. Therefore, the periodic boundary condition of nanotube in circumferential direction changes to open boundary condition (Möbius boundary condition) (Wakabayashi03). The electronic properties of nanoribbons are affected by these open boundaries. In carbon nanotubes, the circumferential periodic boundary condition imposes its electronic properties, making it metallic or semiconducting (Saito92). The electronic properties of nanoribbons, on the other hand, are affected by their open boundaries, as well as their edge geometry. Intrinsically there are dangling bonds at the edges, whose linear combinations form some of the eigenstates near the Fermi energy, and determine the properties of nanoribbons.

The earliest theoretical studies of graphene nanoribbons, using a simple tight-binding method with one π -orbital per atom, predicts that 1/3 of the armchair nanoribbons, whose width index N satisfies $N=3M-1$ (M is an integer), are metallic (Fujita96), and the other 2/3 are semiconductor with band gaps depending on their width, while all zigzag nanoribbons are metallic. This behaviour is similar to characteristics of carbon nanotubes. A characteristic peak is also predicted in the density of states (DOS) of zigzag nanoribbons near Fermi energy (Niimi06; Sasaki06). This peak is a nano-size effect and decreases by increasing the width of nanoribbon. By considering a four-orbitals-per atom tight-binding model, and optimizing the structure of nanoribbons, or simply consider a larger hopping energy for the C-C bonds of the edge in the one-orbital per atom model, the 1/3 rule for armchair nanoribbons does not apply any more, and all the armchair nanoribbons show an energy gap around the Fermi energy. This gap changes with the width of the nanoribbon, which is the effect of the open boundary.

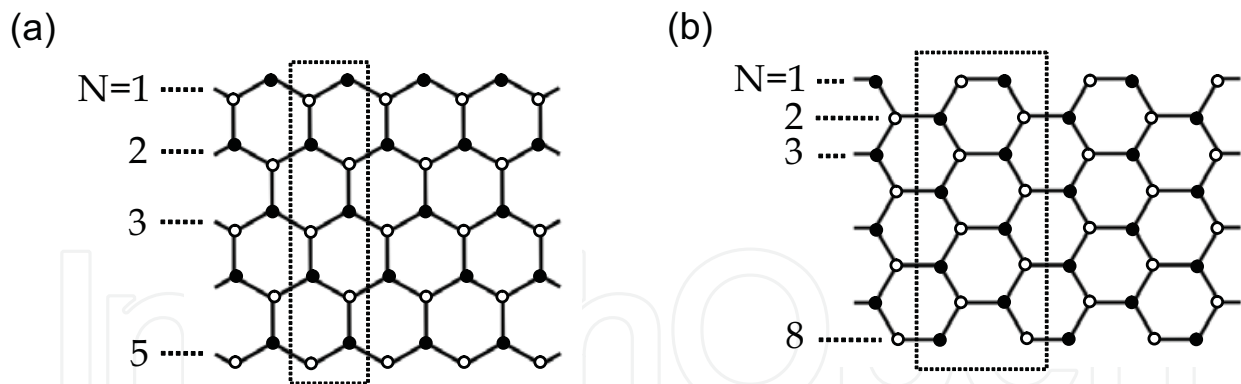


Fig. 1. Graphene nanoribbons with zigzag (a) and armchair (b) edges. The black circles denote sublattice A, while the white circles refer to sublattice B. The dotted rectangle represents the unit cell of the nanoribbon. The width of the nanoribbon is specified by N .

First principle studies based on spin polarized density functional theory (DFT) predicts that all graphene nanoribbons are semiconductors at their ground state with band gaps which depend on their width and edge geometry, closing at infinite width, i. e. infinite graphene (Pisani07). Meanwhile zigzag nanoribbons have localized edge states which are ferromagnetically ordered, but with opposite spin orientation at the two edges which makes them antiferromagnetically coupled. The magnetism in zigzag nanoribbon, a pure carbon system, which arises from π -orbitals of carbon localized at the edge is specially notable (Wakabayashi99).

There are two types of basic site in primitive cell of graphene and the atomic sites of graphene are divided into two sublattices, called A and B. In zigzag nanoribbons the edge atoms belong to the same sublattice, while the two edges carry atoms of two different sublattices. In these nanoribbons, the A-type and B-type atoms are placed alternatively from one edge toward the other one, as shown in Fig. 1(a). The spin in the same sublattice atoms of zigzag nanoribbon is localized in one direction, and in the opposite of the other sublattice. Hence, the total spin of the zigzag nanoribbons is zero, and the edges of the nanoribbons are antiferromagnetically ordered in the ground state. In case of armchair nanoribbons, the edge of the nanoribbon contains both A- and B-type atoms, as dimers, which sit along the edge, as depicted in Fig. 1(b). The black circles in this figure illustrate sublattice A and the white circles refer to sublattice B.

Another important matter in the structure of nanoribbons is the C-C bond lengths with respect to their distance from the edge. There are two types of C-C bonds in a graphene nanoribbon, those which are parallel to the axis of nanoribbon, where we call them type 1, and those which make an 30° or 60° angle with the axis, and we call them type 2. The change of C-C bond length with the number of atomic layers distant from edge are shown in Fig 2 for armchair nanoribbons $N = 8$, and $N = 14$. The 0^{th} layer implies the edge, as shown in the inset. In nanoribbon $N=8$ all C-C bonds are affected by the edge and distort from 1.42 \AA , which is the optimized bond length of graphene. But, for $N=14$, the effect of edge can be seen only till second atomic layer distant from the edge. From the third layer, the bonds are 1.42 \AA , the same as graphene. The bond length of the edge, which is the triple bond, is 1.26 \AA or 1.27 \AA depending on the width of nanoribbon. Patterns of other structures with $N > 14$ are the same as $N = 14$, with edge bond length of 1.26 \AA and the bonds of the bulk are equal to 1.42 \AA .

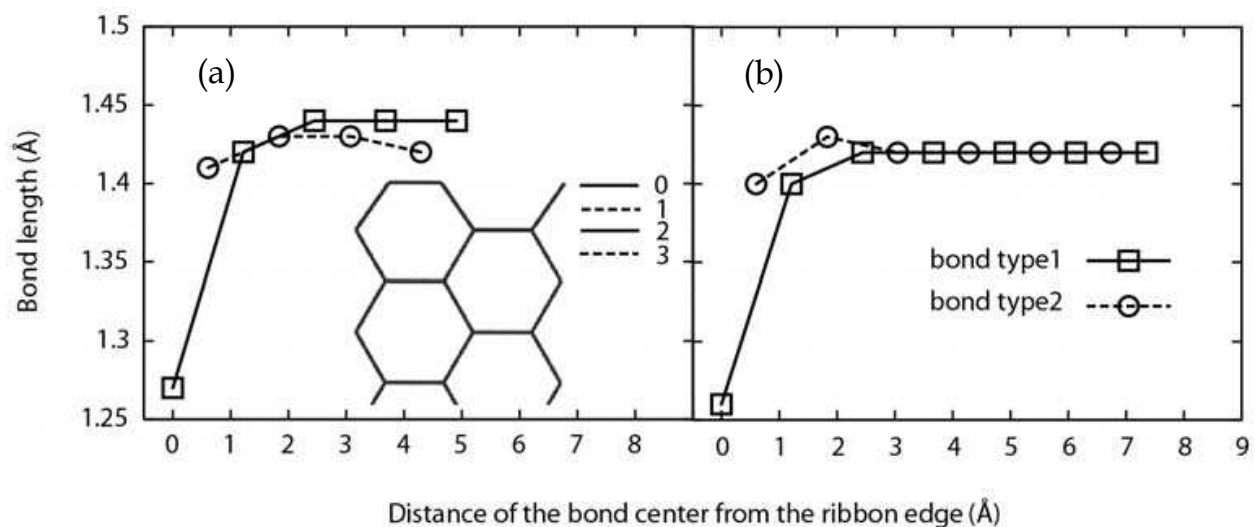


Fig. 2. C-C bond length for different layers of carbon counted as their distance from edge of armchair nanoribbons N=8 (a) and N=14 (b).

3. Tight-binding and NEGF

We use the nonequilibrium Green's function (NEGF) technique to calculate quantum conductance of nanoribbons (Datta95). The electronic structure and forces are obtained through a four-orbitals-per-atom tight-binding model based on semiempirical parameters developed by Xu et al. for carbon (Xu92). This parameterization has been used in tight binding studies of carbon systems, such as fullerenes and nanotubes (Esfarjani98; Ozaki00; Farajian01). We divide the system under study to three parts, as sketched in Fig 3: left lead, conductor, and right lead. According to Landauer formula (Landauer70), the conductance through the conductor region is:

$$C = \frac{2e^2}{h} T, \quad (1)$$

where the coefficient $2e^2/h$ is the conductance quantum in ballistic conductor, and T is the transmission function, and can be expressed in NEGF formalism as follows (Pastawski91, Tian98):

$$T = Tr(\Gamma_L G^r \Gamma_R G^a). \quad (2)$$

Here, Tr indicates the transmission per energy channel between the leads, Γ_L and Γ_R are the coupling functions to the left and right leads, and G^r and G^a are the retarded and advanced Green's functions of the conductor (Torelli00), respectively, given by:

$$G^r = (EI - H - \Sigma^r)^{-1}, \quad (3)$$

$$G^a = [G^r]^\dagger. \quad (4)$$

The advanced Green's function is the Hermitian conjugate of the retarded Green's function. The Green's function describes the dynamics of the electron inside the system. Here, H is the

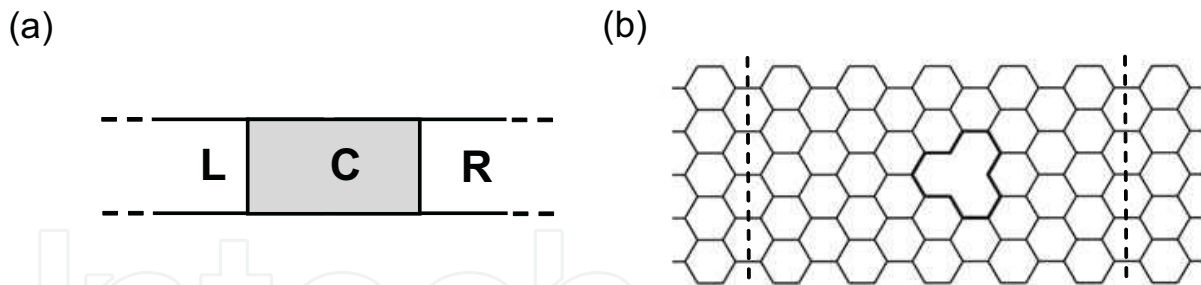


Fig. 3. (a) Schematic picture of a conductor (C) sandwiched between left (L) and right (R) contacts. (b) An armchair nanoribbon $N=11$ including a vacancy defect as an example of the L-C-R system.

Hamiltonian of conductor part, E is the (complex) energy of conducting electron ($E = \varepsilon + i\eta$), with η arbitrarily small, and I is the identity matrix. Σ^r is the retarded self-energy which contains the self-energy of the Left and Right leads, $\Sigma^r = \Sigma_L^r + \Sigma_R^r$, where Σ_L^r and Σ_R^r are obtained from surface Green's functions of the leads as follows (Munoz87):

$$\Sigma_L^r = H_{LC}^\dagger G_L^0 H_{LC} \quad (5)$$

$$\Sigma_R^r = H_{CR} G_R^0 H_{CR}^\dagger \quad (6)$$

where G_L^0 and G_R^0 are the surface Green's functions of the semi-infinite Left and Right leads, respectively; and H_{LC} and H_{CR} represent the coupling matrices to the leads. In fact, the semi-infinite leads are mapped into complex self-energies. The imaginary part of the self-energy implies that the eigenstates are not confined leak from the boundaries. The surface Green's function, which includes the effect of the semi-infinite lead projected at its surface layer, is calculated by López Sancho algorithm (Lopez Sancho84).

The Hamiltonian of the whole system can be written in tight-binding block matrix as follows:

$$H = \begin{pmatrix} H_L & H_{LC} & 0 \\ H_{LC}^\dagger & H_C & H_{CR} \\ 0 & H_{CR}^\dagger & H_R \end{pmatrix}. \quad (7)$$

where H_C is the Hamiltonian of the conductor part, which is used in the Green's function in eq. 3. The coupling functions of the leads, Γ_L and Γ_R , are identified by

$$\Gamma_{L(R)} = i[\Sigma_{L(R)}^r - \Sigma_{L(R)}^a], \quad (8)$$

where Σ^a is the Hermitian conjugate of Σ^r .

In eq. 3, the Hamiltonian, the Green's function, and the self-energies are all represented by matrices, using the tight-binding basis. In the tight-binding expression for carbon used in this work, there are four orbitals representing the $2s$ and $2p$ orbitals of carbon. Hence, for a system with N carbon atoms, the basis set contains $4N$ elements, and the matrices are $4N \times 4N$. In this formalism DOS is equal to $-Im[Tr(G)]/\pi$, where Im indicates the imaginary part.

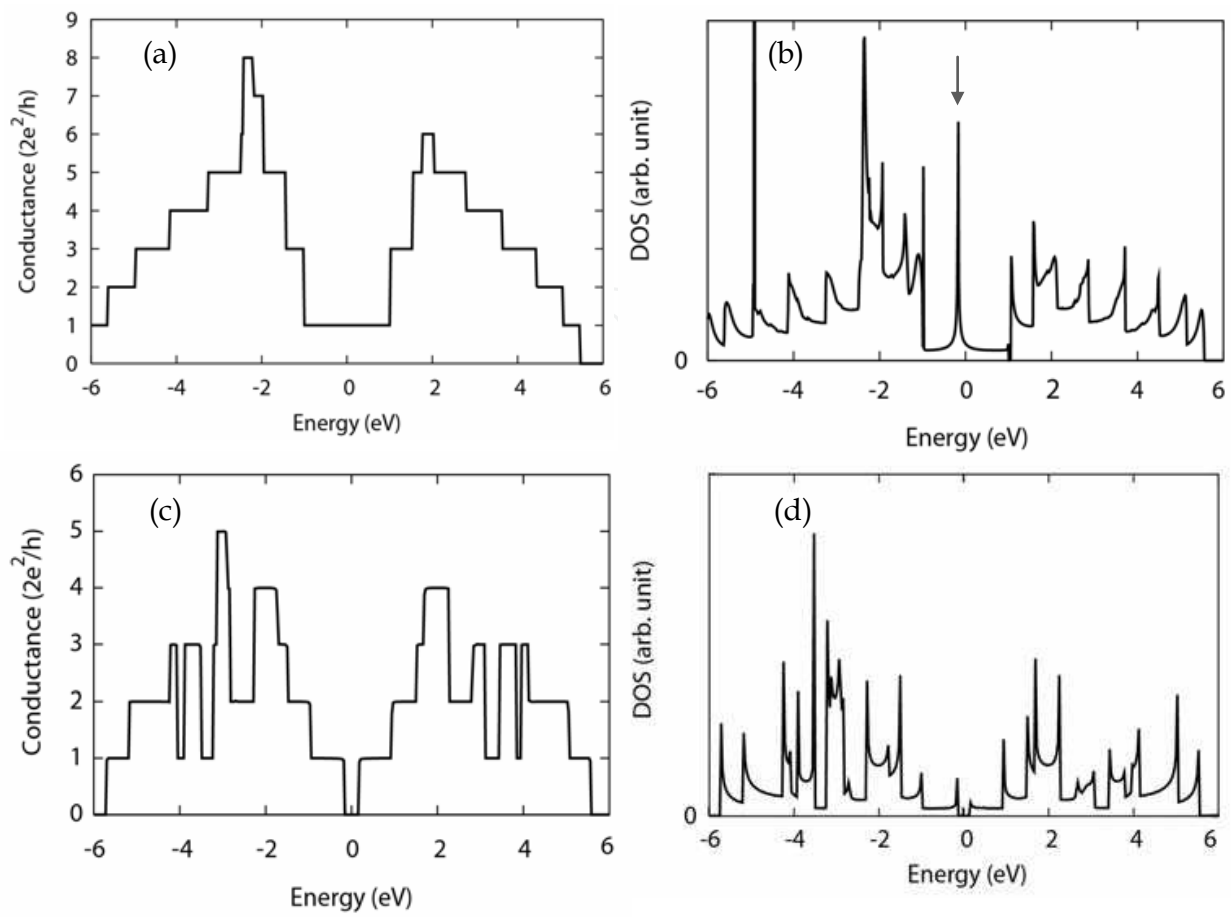


Fig. 4. (a) Conductance and (b) DOS of a zigzag nanoribbon $N=6$. (c) Conductance and (d) DOS of an armchair nanoribbon $N=8$. The Fermi energy is set to zero. The sharp peak specified by an arrow in (a) refers to edge state of the zigzag nanoribbons.

In order to calculate the conductance, the first step is to optimize the geometry of the structure, using the tight-binding description parameterized by Xu et al. (Xu92), to obtain the Hamiltonian description of the system. Then, we calculate the Green's function of the conductor, which includes the effect of the leads through their self-energies. The conductance is then obtained through eq. 1, 2. We do not consider the spin of electrons in the calculations of this chapter, and take part the charge of the carriers in the transport properties. The edges in all structures are pure carbon and are not hydrogen saturated. Figure 4 illustrates the conductance and DOS of a zigzag $N=6$ and an armchair nanoribbon $N=8$, versus the energy of carrier. The Fermi energy of the structures is set to zero. Zigzag nanoribbons with width $N=6$ has metallic behaviour within tight-binding approximation. The sharp peak at the energy 0.18 eV in the DOS, specified by an arrow in Fig. 4(b), refers to localized edge states of zigzag nanoribbons. These edge states correspond to the non-bonding π orbitals. The existence of these edge states has been confirmed by experimental observations also (Niimi06). The edge states are the characteristics of zigzag nanoribbons and do not appear in the armchair edges. The conductance and DOS of the armchair nanoribbons shows an energy gap around Fermi energy. This energy gap depends on the width of the nanoribbons and decreases by increasing the width. In graphene, the in-plane bonds are the σ bonds with sp^2 hybridization, which does not contribute in conduction.

These are the π bonds, perpendicular to nanoribbon surface, which are responsible for the conduction. The change in bond length results in a change in overlap of Pz orbitals, i.e. the π bonds, and leads to changing the conduction property. For those nanoribbons whose π pattern is distorted more from the graphene sheet, the energy gap is larger. Regardless of appropriate boundary condition, it seems that the typical bond length of 1.42\AA is the most suitable for π orbitals to contribute in conduction. It is worth mentioning that saturation of the edge by hydrogen reduces the gap, but does not remove it. The energy gap of armchair nanoribbons $N=8$, for instance, decreases from 0.45 eV to 0.27 eV by hydrogen saturation of the edge.

4. Quantum conductance of nanoribbons with structural defects

For calculating the conductance of nanoribbons with defects we consider five unit cells of the nanoribbon as the conductor part, which is sandwiched between two semi-infinite contacts, as sketched in Fig 3(b). The contacts are defectless graphene nanoribbons with the same width and edge geometry of the middle junction.

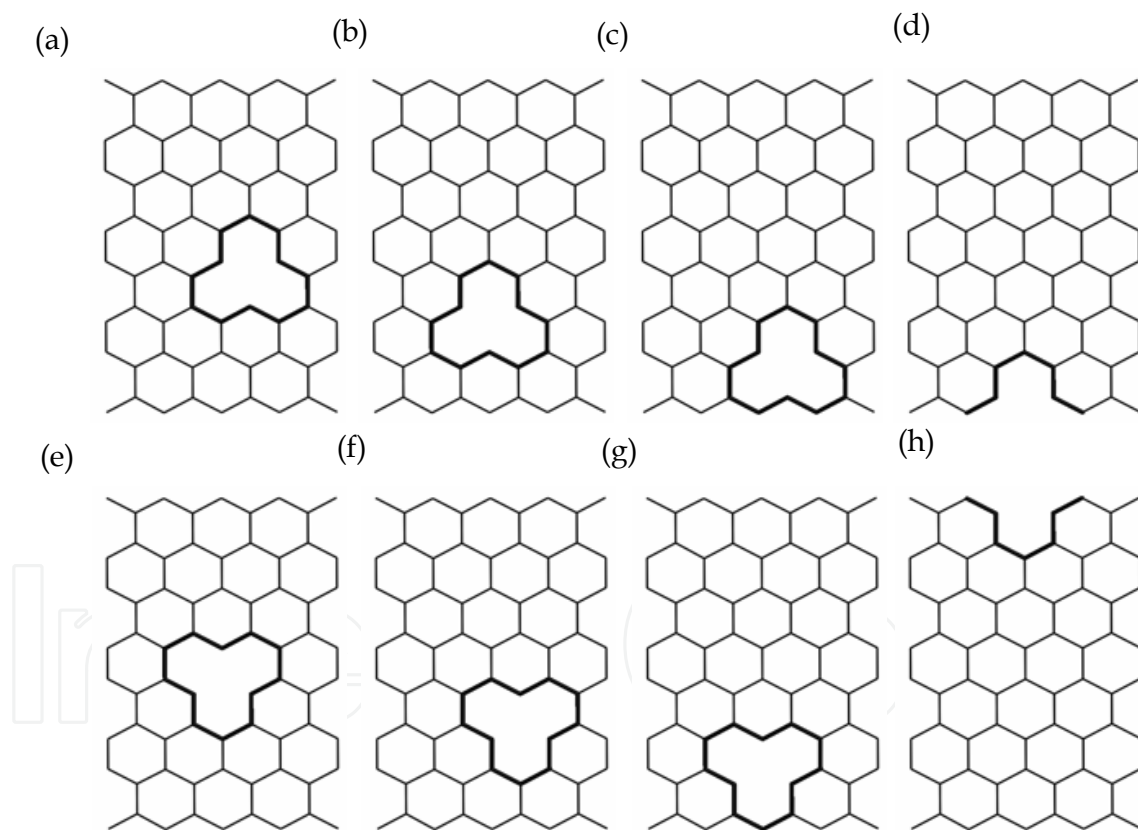


Fig. 5. Zigzag nanoribbons $N=8$ with vacancies of type B (top) and type A (bottom) at different positions toward the edge.

In order to obtain the Hamiltonian of the middle junction, i.e. conductor, the nanoribbon is sandwiched between five unit cells of nanoribbons with the same width from left and right and the structure is optimized, such that the maximum force on each atom is less than 0.01 eV/\AA (Gorjizadeh09). After the optimization, the five extra unit cells on each of the two sides of the nanoribbons are eliminated, and the five unit cells of the nanoribbon left in the

middle are used as the junction part for calculations of conductance. Using this method, the extra unit cells which were eliminated, omit the effects of open boundary along the axis, such that the junction part represents a portion of an infinite nanoribbon. The geometries of the semi-infinite left and right contacts are also extracted from the relaxed structures, obtained the same way as the junction part. This way, we are able to simulate the effect of a single defect in the junction part, without having periodic boundary condition.

The vacancy defect can appear in the site of an atom of type A or type B in the nanoribbon. The position and type of vacancy, A or B, versus the edge of the nanoribbon is the matter of considering in the calculations.

4.1 Defects in zigzag nanoribbons

We consider a zigzag nanoribbon $N=8$ with five unit cells in the middle and calculate the conductance when there is a vacancy of type A and B at different positions versus edge, as illustrated in Fig. 5. First we consider the structure of Fig. 5(a), a vacancy of type B in the middle of the nanoribbon. Figure 6 depicts the calculated conductance of nanoribbon with this defect, compared with the conductance of a perfect (defectless) nanoribbon. It can be noticed from this figure that number of conducting channels decreases in the defected nanoribbon. By moving the position of this vacancy from center toward the edge which has the same type of atom, according to Fig. 5(a-d), the conductance near the Fermi energy is changed (Fig. 6(b)). The behaviour of the conductance clearly depends on the place of the vacancy versus the edge. When the vacancy is in the middle of the nanoribbon, the conductance at Fermi energy decreases to zero. By moving the vacancy from the center toward the edge, the conductance near the Fermi energy increases until it reaches the conductance of a perfect nanoribbon, when the vacancy is at the edge. The energy for which the decrease of conductance is the strongest is slightly below the Fermi energy, around -0.18 eV. On the other hand, the vacancy of type A in the center of the nanoribbon, as in Fig. 5(e), even opens a gap around the energy -0.18 eV (Fig. 6(c)). Moving the place of this vacancy toward the same edge, according to Fig. 5(e-g), will result in the same trend as vacancy B, as depicted in Fig. 6(d). As mentioned in section 2, all zigzag nanoribbons have a typical peak in their DOS near and slightly below the Fermi energy which is due the edge states. Our results show that a vacancy defect inside the nanoribbon affects the edge states of the nanoribbon. By removing one atom from the lattice of the nanoribbon, three sp^2 bonds are broken, creating three dangling bonds in the neighboring carbon atoms. These dangling bonds tend to spread toward the neighboring carbon atoms of the nanoribbon in order to overlap with electronic orbitals of their neighbors and lower their energy. Hence, the electronic wave functions near the vacancy are affected. In other words, some localized states appear in the vicinity of the vacancy and affect the π bonds of the nanoribbon. Therefore, the effect of the vacancy on the π bands (from -1 to 1 eV in Fig. 6(b)), which are responsible for conduction near the Fermi energy, is significant. If the localized vacancy states are in the middle of the nanoribbon, their effect on the whole electronic wave function will be maximum. As the width of the nanoribbon is small, on the order of a few Å, the effect of the localized states of the vacancy are spread until both nanoribbon edges. Once the vacancy is moved toward one edge, the effect of the localized vacancy states at and near the other edge will decrease, due to increase of the distance between the vacancy and the other edge of the nanoribbon. Therefore, the number of less affected conducting channels of the nanoribbon increases compared to when the vacancy is in the middle of nanoribbon.

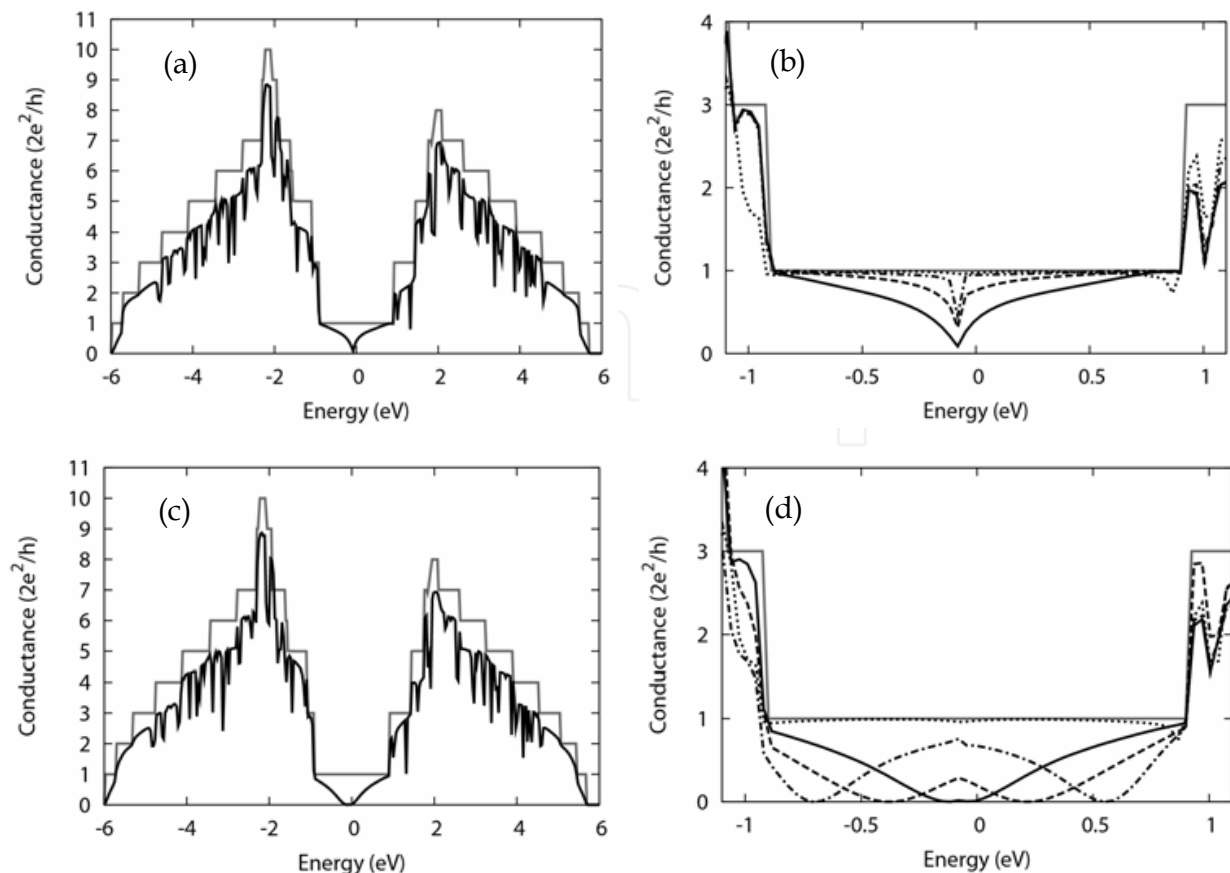


Fig. 6. Conductance of a zigzag nanoribbon $N=8$ with (a) vacancy defect of Fig. 5(a) compared with the defectless nanoribbon sketched in gray, (b) vacancy defects of type B at different positions from the edge. The solid line is defect of Fig. 5(a), dashed line is defect of Fig. 5(b), dashed-dotted line is defect of Fig. 5(c), and dotted line is defect of Fig. 5(d). Conductance of the same zigzag nanoribbon $N=8$ with (c) vacancy defect of Fig. 5(e) compared with the defectless nanoribbon sketched in gray. (d) Vacancy defects of type A at different positions from the edge. The solid line is defect of Fig. 5(e), dashed line is defect of Fig. 5(f), dashed-dotted line is defect of Fig. 5(g), and dotted line is defect of Fig. 5(h).

The same situation happens for zigzag nanoribbons with other widths, such as $N=6$ and $N=4$. However, the gap opening around the energy -0.18 eV when the vacancy is in the middle of the nanoribbon, is larger when the width of the nanoribbon is smaller. This gap is equal to 1.0 eV for the nanoribbon $N=4$, while it is 0.35 eV for the nanoribbon $N=8$. Therefore, by increasing the width of nanoribbon, this effect will diminish.

Next, we place an adatom at a nearest neighbor position of vacancy. An adatom-vacancy defect of this kind is more stable than one adatom and one vacancy defect (Hashimoto04). A carbon adatom is not stable on graphene. It will diffuse on graphene with a diffusion barrier of 0.14 eV (Lehtinen03; Hashimoto04) It appears mostly in the vicinity of the vacancies, because this combination of vacancy and neighboring adatom has been predicted to be metastable and long lived (Hashimoto04; Krasheninnikov01; Lu04).

An adatom can be attached on top of an A-type or a B-type site. Figure 7(a-b) shows schematic of the adatom-vacancy defect, when adatom is in site A or B at a nearest neighboring site of a vacancy type A in zigzag nanoribbon $N=6$. The C-C bond between the

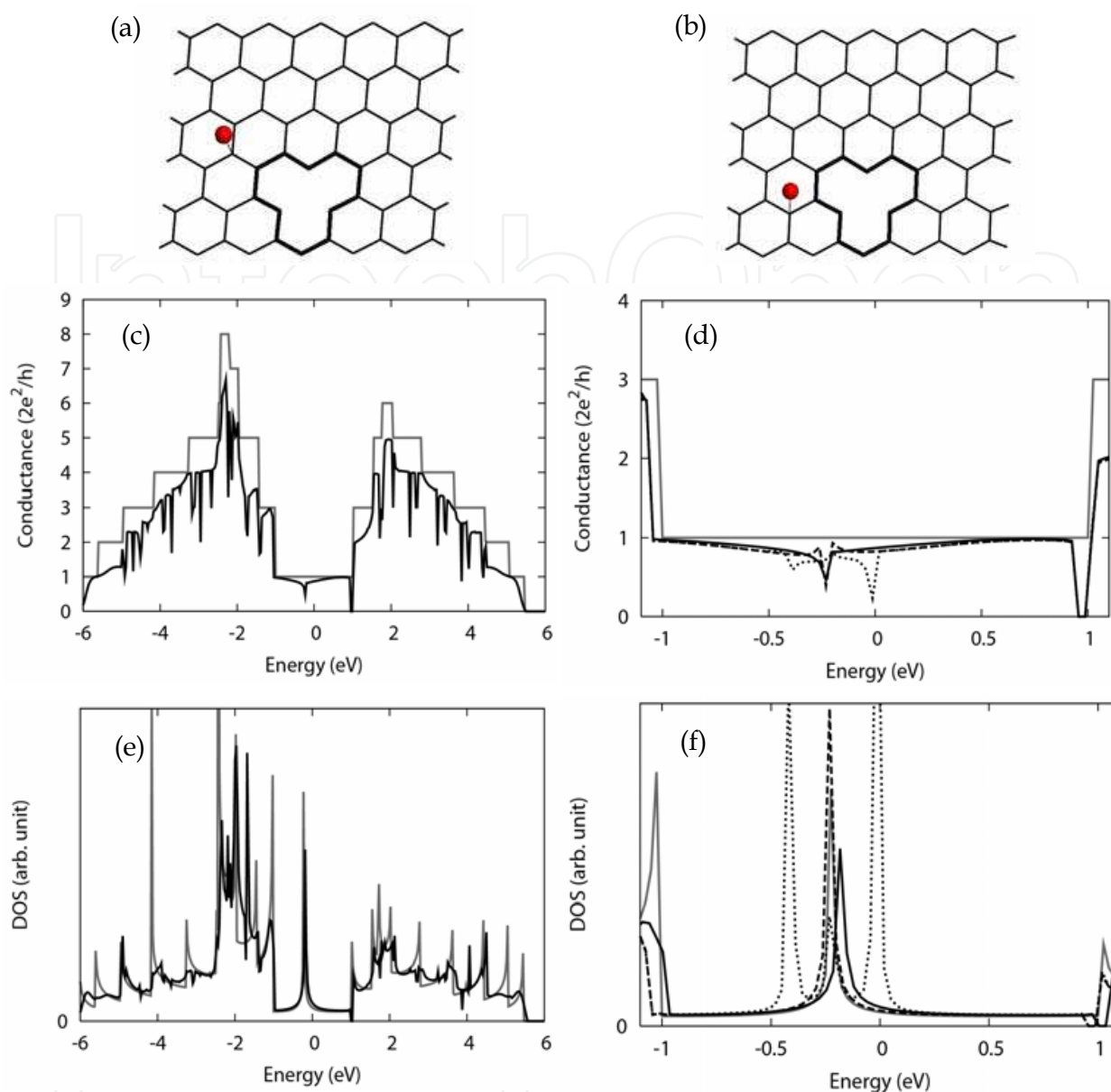


Fig. 7. Schematic of a zigzag nanoribbon $N=6$ with adatom-vacancy defect, when adatom is in (a) site A or, (b) site B, in vicinity of a vacancy type A. (c) Conductance of the zigzag nanoribbon with vacancy type A. (d) Comparison of the conductance of plot (c) with adatom-vacancy defects of (a) and (b). The solid line is the conductance of vacancy type A, dashed line is that of adatom-vacancy type A-A (Fig. 5(a)), and dotted line is that of adatom-vacancy type B-A. Two peaks appear near and at the two sides of the original peak of the nanoribbon, in case of adatom-vacancy type B-A, indicating that localized states appear at these energies.

adatom and the carbon atom of the nanoribbon is 2.04 \AA which indicates that the adatom is physisorbed on the nanoribbon. Conductance of the zigzag nanoribbon $N=6$ with the vacancy is sketched in Fig. 7.c, while the conductance of adatom-vacancy defects of type A-A and B-A are shown in Fig. 7.d. The results of DOS in Fig. 7. e-f show that two peaks appear near and at the two sides of the original peak of the nanoribbon, in case of adatom-vacancy type B-A, indicating that localized states appear at these energies which are located

at energy intervals -0.18 eV and $+0.21$ eV away from the original peak. These two energies show a drastic drop, instead of the drop at the energy of the original peak at -0.18 eV. However, the DOS and conductance of adatom of type A near vacancy of type A does not change compared to that of vacancy A defect. Therefore, the adatom does not change the transport property of the zigzag nanoribbon when it is attached to a site of the same type as vacancy, while it splits the original peak of the DOS at -0.18 eV and decreases the conductance when it is attached to a site of different type site compared to the vacancy. The same results were obtained for zigzag nanoribbons of other widths, i. e. $N=4$ and 8 .

4.2 Defects in armchair nanoribbons

We consider the same defects of the vacancy and adatom-vacancy in the structures of armchair nanoribbons $N=8$, 12 , and 16 , and compare the conductance characteristics with those of perfect structures. Armchair nanoribbons are semiconducting. Figure 8(a-b) shows the conductance of an armchair nanoribbon $N=8$ with a vacancy type B in the middle of the nanoribbon, and its comparison with those of structures with one and two atom vacancy at the edge. Similar to the zigzag nanoribbons, in armchair nanoribbons also localized states appear when there is vacancy in their structures, and the conductance decreases due to defects compared with the perfect nanoribbon. But the energy gap is not affected by the defects. This could be expected as the gap arises owing to the lack of conducting channels (bands), for that particular energy interval, within the two semi-infinite defectless contacts. The vacancy states are localized near the vacancy within the junction part, which attaches the two semi-infinite graphene contacts. These localized states cannot generate extra bands within the contacts, and therefore the gap remains upon introducing the vacancy.

Figure 8(c-d) depicts the conductance and DOS of adatom-vacancy defects. The conductance of adatom-vacancy is the same as that of vacancy defect, indicating that adatom does not affect the transport properties of the armchair nanoribbon, both for the adatom and vacancy of the same type and different types. The same results are obtained for the nanoribbons $N=12$ and 16 . This effect is attributed to the lack of edge state in armchair nanoribbon. The edge state in zigzag nanoribbon produces a peak in DOS at -0.18 eV. This peak is split into two by different sites of adatom-vacancy defects, as is shown in Fig. 7(f). With the absence of edge-state peak in armchair nanoribbons, the split does not occur and the conductance of adatom-vacancy defect is similar to that of vacancy.

5. Conclusion

We study the effect of defects such as vacancy and adatom-vacancy on the conductance of graphene nanoribbons. Our results show that localized states appear when there is vacancy inside the nanoribbon, which affects its conductance. The drop of conductance depends on the place of the vacancy. When the vacancy is at the middle of the nanoribbon, its effect on conductance at energies near Fermi energy is maximum. For zigzag nanoribbons, there is a drastic drop of conductance at the energy -0.18 eV which is the energy of the original peak in the density of states (DOS) of the nanoribbon. A gap opens around this energy, whose width depends on the width of the nanoribbon: The thinner the nanoribbon, the wider the gap. By moving the vacancy from the middle of the nanoribbon toward the edge, the decrease of

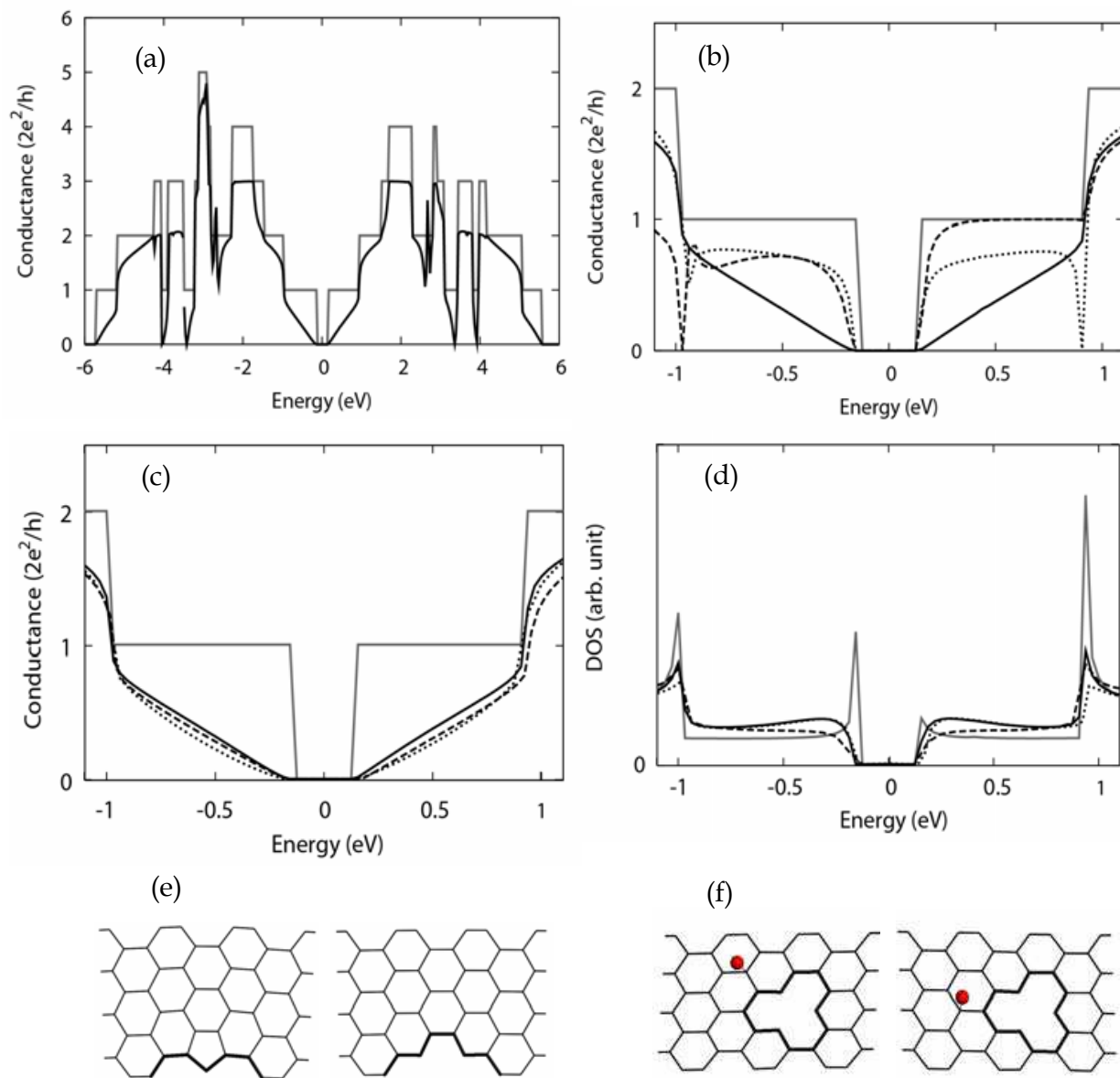


Fig. 8. (a) Conductance of an armchair nanoribbon $N=8$ with the vacancy type B. (b) Comparison of the conductance of plot (a) with those of the nanoribbon with one and two atom vacancy at the edge (structures of (e)). (c) Comparison of the conductance of plot (a) with those of adatom-vacancy defects of type A-A and B-B (structures of (f)).

conductance is lowered, and it reaches zero when the vacancy is at the edge, i. e. the conductance is the same as that of a perfect nanoribbon. Binding of a carbon adatom with a carbon atom near vacancy results in two extra peaks in the DOS near the Fermi energy of zigzag nanoribbons. This binding makes localized states at energies of the new peaks and results in the decrease of conductance at these energies. These effects are very sensitive to the adatom and vacancy types and their relative distances. The peak splitting in the DOS of zigzag nanoribbons occurs when adatom and vacancy are of different types. In the case of thin armchair nanoribbons, which are semiconducting, the presence of vacancy and adatom-vacancy defects decreases the number of conducting channels, but the gap does not change due to these defects. The vacancy and adatom-vacancy defects have the same effect on

conductance owing to the absence of edge state near the Fermi energy of armchair nanoribbons. We neglected the spin of electrons in all the calculations in this chapter, and considered the electronic conductance through tight-binding formalism.

6. Acknowledgments

The authors would like to express their sincere thanks to the crew of the Center for Computational Materials Science, Institute for Materials Research, for their support of the Hitachi SR11000 (model K2) supercomputer system and also Global COE program of Tohoku University for financial support.

7. References

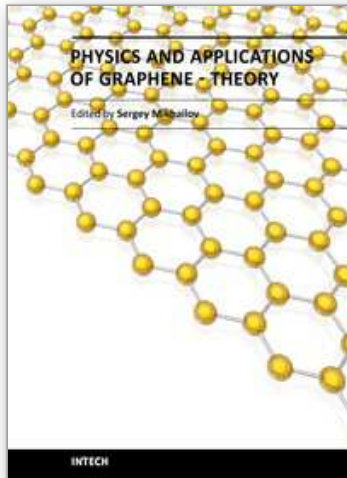
- [Datta, 1995] Datta, S. (1995). *Electronic transport in mesoscopic systems*, Cambridge University Press, ISBN, 0-521-41604-3, Cambridge, UK
- [Esfarjani et al., 1998] Esfarjani, K.; Hashi, Y.; Onoe, J.; Takeuchi, K. & Kawazoe, Y. Vibrational modes and IR analysis of neutral photopolymerized C₆₀ dimers. *Physical Review B*, Vol. 57, No. 1, (1998), pp. 223-229
- [Farajian & Mikami, 2001] Farajian, A. A. & Mikamai, M. Electronic and mechanical properties of C₆₀-doped nanotubes. *Journal of Physics: Condensed Matter*, Vol. 13, (3 September 2001), pp. 8049-8059
- [Fujita et al., 1996] Fujita, M.; Wakabayashi, K.; Nakada, K. & Kusakabe, K. Peculiar localized state at zigzag graphite edge. *Journal of the Physical Society of Japan*, Vol. 65, No. 7, (1996), pp. 1920-1923
- [Gorjizadeh et al., 2008] Gorjizadeh, N.; Farajian, A.A.; Esfarjani, K. & Kawazoe, Y. Spin and band-gap engineering in doped graphene nanoribbons. *Physical Review B*, Vol. 78, (2008), Article ID 155427, 6 pages
- [Gorjizadeh et al., 2009] Gorjizadeh, N.; Farajian, A. A. & Kawazoe, Y. Effects of defects on conductance of graphene nanoribbons. *Nanotechnology* Vol. 20, (2009), Article ID 015201, 6 pages
- [Gunlycke et al., 2007] Gunlycke, D.; Li, J.; Mintmire, J. W. & White, C. T. Altering low-bias transport in zigzag edge graphene nanostrips with edge chemistry. *Applied Physics Letters*, Vol. 91, No. 11, (2007), Article ID 112108, 3 pages
- [Hashimoto et al., 2004] Hashimoto, A.; Suenaga, K.; Gloter, A.; Urita, K. & Iijima, S. Direct evidence for atomic defects in graphene layers. *Nature*, Vol. 430, No.7002, (19 August 2004), pp. 870-873
- [Hod et al., 2007] Hod, O.; Barone, V.; Peralta, J. E. & Scuseria, G. E. Enhanced half-metallicity in edge oxidized zigzag graphene nanoribbons *Nano Letters*, Vol. 7, No. 8, (2007), pp. 2295-2299
- [Hod & Scuseria, 2009] Hod O. & Scuseria, G. E. Electromechanical properties of suspended graphene nanoribbons. *Nano Letters*, Vol. 9, No. 7, (2009), pp. 2619-2622
- [Huang et al., 2007] Huang, B.; Yan, Q.; Zhou, G.; Wu, J.; Gu, B.-L.; Duan, W. & Liu, F. Making a field effect transistor on a single graphene nanoribbon by selective doping *Applied Physics Letters*, Vol. 91, No. 25, (2007), Article ID 253122, 3 pages

- [Klein, 1994] Klein, D. J. Graphitic polymer strips with edge states. *Chemical Physics Letters*, Vol. 217, No. 3, (1994), pp. 261-265
- [Kobayashi et al., 2005] Kobayashi, Y.; Fukui, K.-I.; Enoki, T.; Kusakabe, K. & Y. Kaburagi. Observation of zigzag and armchair edges of graphite using scanning tunneling microscopy and spectroscopy. *Physical Review B*, Vol. 71, No. 19, (2005), Article ID 193406, 4 pages
- [Krasheninnikov et al., 2001] Krasheninnikov, A. V.; Nordlund, K.; Sirviö, M.; Salonen, E. & Keinonen, J. Formation of ion-irradiation-induced atomic-scale defects on walls of carbon nanotubes. *Physical Review B*, Vol. 63, No. 24, (2001), Article ID 245405, 6 pages
- [Landauer, 1970] Landauer, R. Electrical resistance of disordered one-dimensional lattices. *Philosophical Magazine*, Vol. 21, No. 172, (1970), pp. 863-872
- [Lehtinen et al., 2003] Lehtinen, P. O.; Foster, A.S.; Ayuela, A.; Krasheninnikov, A.; Nordlund, K. & Nieminen, R. M. Magnetic properties and diffusion of adatoms on graphene sheet. *Physical Review Letters*, Vol. 91, No. 1, (4 July 2003), Article ID 17202, 4 pages
- [Li et al., 2008] Li, Z.; Qian, H.; Wu, J.; Gu, B.-L. & Duan, W. Role of symmetry in the transport properties of graphene nanoribbons under bias. *Physical Review Letters*, Vol. 100, No. 20, (2008), Article ID 206802, 4 pages
- [Lopez Sancho et al., 1984] Lopez Sancho, M. P.; Lopez Sancho, J. M. & Rubio, J. Quick iterative scheme for the calculation of transfer matrices: application to Mo (100). *Journal of Physics F: Metal Physics*, Vol. 14, No. 5, (1984), pp. 1205-1216
- [Lu & Pan, 2004] Lu, A. J. & Pan, B.C. Nature of single vacancy in achiral carbon nanotubes. *Physical Review Letters*, Vol. 92, No. 10, (2004), Article ID 105504, 4 pages
- [Munoz et al., 1987] Munoz, M. C.; Velasco, V. R. & Garcia-Moliner, F. Tight binding models for non ideal semiconductor interfaces. *Progress in Surface Science*, Vol. 26, No. 1-4, (1987), pp. 117-133
- [Maruyama et al., 2004] Maruyama, M.; Kusakabe, K.; Tsuneyuki, S.; Akagi, K.; Yoshimoto, Y. & Yamauchi, J. Magnetic properties of nanographite with modified zigzag edges. *Journal of Physics and Chemistry of Solids*, Vol. 65, No. 2-3, (2004), pp. 119-122
- [Niimi et al., 2005] Niimi, Y.; Matsui, T.; Kambara, H.; Tagami, K.; Tsukada, M. & Fukuyama, H. Scanning tunneling microscopy and spectroscopy studies of graphite edges. *Applied Surface Science*, Vol. 241, No. 1-2, (2005), pp. 43-48
- [Niimi et al., 2006] Niimi, Y.; Matsui, T.; Kambara, H.; Tagami, K.; Tsukada, M. & H. Fukuyama. Scanning tunneling microscopy and spectroscopy of the electronic local density of states of graphite surfaces near monoatomic step edges. *Physical Review B*, Vol. 73, No. 8, (2006), Article ID 085421, 8 pages
- [Novoselov et al., 2004] Novoselov, K. S.; Geim, A. K.; Morozov, S. V.; Jiang, D.; Zhang, Y.; Dubonos, S. V.; Grigoreiva, I. V. & Firsov A. A. Electric field effect in atomically thin carbon films. *Science*, Vol. 306, No. 5696, (2004), pp. 666-669
- [Novoselov et al., 2005] Novoselov, K. S.; Geim, A. K.; Morozov S. V. et al. Two dimensional gas of massless Dirac fermions in graphene. *Nature*, Vol. 438, No. 7065, (2005), pp. 197-200

- [Obradovic et al., 2006] Obradovic, B.; Kotlyar, R.; Heinz, F. et al. Analysis of graphene nanoribbons as a channel material for field-effect transistors. *Applied Physics Letters*, Vol. 88, No. 14, (2006), Article ID 142102, 3 pages
- [Ozaki et al., 2000] Ozaki, T.; Iwasa, Y. & Mitani, T. Stiffness of single-walled carbon nanotubes under large strain. *Physical Review Letters*, Vol. 84, No. 8, (2000), pp. 1712-1715
- [Pastawski , 1991] Pastawski, H. M. Classical and quantum transport from generalized Landauer-Büttiker equations. *Physical Review B*, Vol. 44, No. 12, (1991), pp. 6329-6339
- [Pisani et al., 2007] Pisani, L.; Chan, J. A.; Montanari, B. & Harrison, N. M. Electronic structure and magnetic properties of graphitic ribbons. *Physical Review B*, Vol. 75, No. 6, (2007), Article ID 064418, 9 pages
- [Saito et al., 1992] Saito, R.; Fujita, M.; Dresselhaus, G. & Dresselhaus, M. S. Electronic structure of chiral graphene tubules. *Applied Physics Letters*, Vol. 60, No. 18, (1992), pp. 2204-2206
- [Sasaki et al., 2006] Sasaki, K.; Murakami, S. & R. Saito. Stabilization mechanism of edge states in graphene. *Applied Physics Letters*, Vol. 88, No. 11, (2006), Article ID 113110, 3 pages
- [Sols et al., 2007] Sols, F.; Guinea, F. & Neto, A. H. C. Coulomb blockade in graphene nanoribbons. *Physical Review Letters*, Vol. 99, No. 16, (2007), Article ID 166803, 4 pages
- [Son et al., 2006] Son, Y.-W.; Cohen, M. L. & Louie, S. G. Energy gaps in graphene nanoribbons. *Physical Review Letters*, Vol. 97, No. 21, (2006), Article ID 216803, 4 pages
- [Son et al., 2006] Son, Y.-W.; Cohen, M. L. & Louie, S. G. Half-metallic graphene nanoribbons. *Nature*, Vol. 444, No. 7117, (2006), pp. 347-349
- [Tian et al., 1998] Tian, W.; Datta, S.; Hong, S.; Reifenberger, R.; Henderson, J. I. & Kubiak, C. P. Conductance spectra of molecular wires. *The Journal of Chemical Physics*, Vol. 109, No. 7, (15 August 1998), pp. 2874-2882
- [Torelli & Mitas, 2000] Torelli, T. & Mitas, L. Electron Correlation in C_{4N+2} Carbon Rings: Aromatic versus Dimerized Structures. *Physical Review Letters*, Vol. 85, No. 8, (2000), pp. 1702-1705
- [Wakabayashi et al., 1999] Wakabayashi, K.; Fujita, M.; Ajiki, H. & Sigrist, M. Electronic and magnetic properties of nanographite ribbons. *Physical Review B*, Vol. 59, No. 12, (1999), pp. 8271-8282
- [Wakabayashi & Harigaya, 2003] Wakabayashi, K. & Harigaya, K. Magnetic Structure of Nano-Graphite Möbius Ribbon. *Journal of the Physical Society of Japan*, Vol. 72, No. 5, (May 2003), pp. 998-1001
- [Wu et al., 2010] Wu, M. H.; Pei, Y. & Zeng, X. C. Planar tetracoordinate carbon strips in edge decorated graphene nanoribbon *Journal of the American Chemical Society*, Vol. 132, No. 16, (2010), pp. 5554-5555
- [Xu et al., 1992] Xu, C. H.; Wang, C. Z.; Chan, C. T. & Ho, K. M. A transferable tight-binding potential for carbon. *Journal of Physics: Condensed Matter*, Vol. 4, No. 28, (13 July 1992), pp. 6047-6054

- [Yan et al., 2007] Yan, Q.; Huang, B.; Yu, J.; Zheng, F.; Zang, J.; Wu, J.; Gu, B.-L.; Liu, F. & Duan, W. Intrinsic current-voltage characteristics of graphene nanoribbons transistors and effect of edge doping. *Nano Letters*, Vol. 7, No. 6, (2007), pp. 1469-1473
- [Zhang et al., 2005] Zhang, Y.; Tan, Y.-W.; Stormer, H. L. & Kim, P. Experimental observation of the quantum Hall effect and Berry's phase in graphene. *Nature*, Vol. 438, No. 7065, (2005), pp. 201-204
- [Zhu et al., 2010] Zhu, L.; Wang, J.; Zhang, T.; Ma, L., Lim, C. W.; Ding, F. & Zeng, X. C. Mechanically robust tri-wing graphene nanoribbons with tunable electronic and magnetic properties. *Nan Letters*, Vol. 10, No. 2, (2010), pp. 494-498

IntechOpen



Physics and Applications of Graphene - Theory

Edited by Dr. Sergey Mikhailov

ISBN 978-953-307-152-7

Hard cover, 534 pages

Publisher InTech

Published online 22, March, 2011

Published in print edition March, 2011

The Stone Age, the Bronze Age, the Iron Age... Every global epoch in the history of the mankind is characterized by materials used in it. In 2004 a new era in material science was opened: the era of graphene or, more generally, of two-dimensional materials. Graphene is the strongest and the most stretchable known material, it has the record thermal conductivity and the very high mobility of charge carriers. It demonstrates many interesting fundamental physical effects and promises a lot of applications, among which are conductive ink, terahertz transistors, ultrafast photodetectors and bendable touch screens. In 2010 Andre Geim and Konstantin Novoselov were awarded the Nobel Prize in Physics "for groundbreaking experiments regarding the two-dimensional material graphene". The two volumes *Physics and Applications of Graphene - Experiments* and *Physics and Applications of Graphene - Theory* contain a collection of research articles reporting on different aspects of experimental and theoretical studies of this new material.

How to reference

In order to correctly reference this scholarly work, feel free to copy and paste the following:

Narjes Gorjizadeh, Yoshiyuki Kawazoe and Amir A. Farajian (2011). Electronic and Transport Properties of Defected Graphene Nanoribbons, *Physics and Applications of Graphene - Theory*, Dr. Sergey Mikhailov (Ed.), ISBN: 978-953-307-152-7, InTech, Available from: <http://www.intechopen.com/books/physics-and-applications-of-graphene-theory/electronic-and-transport-properties-of-defected-graphene-nanoribbons>

INTECH
open science | open minds

InTech Europe

University Campus STeP Ri
Slavka Krautzeka 83/A
51000 Rijeka, Croatia
Phone: +385 (51) 770 447
Fax: +385 (51) 686 166
www.intechopen.com

InTech China

Unit 405, Office Block, Hotel Equatorial Shanghai
No.65, Yan An Road (West), Shanghai, 200040, China
中国上海市延安西路65号上海国际贵都大饭店办公楼405单元
Phone: +86-21-62489820
Fax: +86-21-62489821

© 2011 The Author(s). Licensee IntechOpen. This chapter is distributed under the terms of the [Creative Commons Attribution-NonCommercial-ShareAlike-3.0 License](#), which permits use, distribution and reproduction for non-commercial purposes, provided the original is properly cited and derivative works building on this content are distributed under the same license.

IntechOpen

IntechOpen